

GALEX Discovery of a Damped Ly α System at Redshift $z \approx 1$ ^{1,2}

Eric M. Monier

*Department of Physics, The College at Brockport, State University of New York,
Brockport, NY 14420*

emonier@brockport.edu

and

David A. Turnshek, Sandhya M. Rao, and Anja Weyant

Department of Physics & Astronomy, University of Pittsburgh, Pittsburgh, PA 15260

ABSTRACT

We report the first discovery of a QSO damped Ly α (DLA) system by the *GALEX* satellite. The system was initially identified as a Mg II absorption-line system ($z_{abs} = 1.028$) in the spectrum of SDSS QSO J0203–0910 ($z_{em} = 1.58$). The presence of unusually strong absorption due to metal lines of Zn II, Cr II, Mn II, and Fe II clearly suggested that it might be a DLA system with $N_{HI} \geq 2 \times 10^{20}$ atoms cm⁻². Follow-up *GALEX* NUV grism spectroscopy confirms the system exhibits a DLA absorption line, with a measured H I column density of $N_{HI} = 1.50 \pm 0.45 \times 10^{21}$ atoms cm⁻². By combining the *GALEX* N_{HI} determination with the SDSS spectrum measurements of unsaturated metal-line absorption due to Zn II, which is generally not depleted onto grains, we find that the system’s neutral-gas-phase metal abundance is $[Zn/H] = -0.69 \pm 0.22$, or $\approx 20\%$ solar. By way of comparison, although this system has one of the largest Zn⁺ column densities, its metal abundances are comparable to other DLAs at $z \approx 1$. Measurements of the abundances of Cr, Fe, and Mn help to further pin down the evolutionary state of the absorber.

Subject headings: galaxies: formation — galaxies: evolution — quasars: absorption lines — quasars: SDSS J0203–0910

¹Based on observations made with the NASA Galaxy Evolution Explorer. GALEX is operated for NASA by the California Institute of Technology under NASA contract NAS5-98034.

²Based in part on data obtained from the Sloan Digital Sky Survey.

1. Introduction

Since the first survey for damped $\text{Ly}\alpha$ systems (DLAs) by Wolfe et al. (1986), it has been recognized that these galaxy-sized columns of neutral hydrogen ($N_{\text{HI}} \geq 2 \times 10^{20}$ atoms cm^{-2}) trace the neutral gas content of the universe back to the epoch of the earliest QSOs. Spectroscopic surveys for DLAs rely on only the presence of a background QSO, and therefore probe the universe independently of normal galaxy imaging. As such, they do not depend on the luminosity or spectral energy distribution of any associated galaxies. Only the presence of significant dust in the absorber would cause a bias against the identification of a DLA system. Surveys have shown that DLAs trace the bulk of the observable H I gas mass in the universe (Prochaska, Herbert-Fort, & Wolfe 2005; Rao, Turnshek, & Nestor 2006, hereafter RTN2006).

Several facets of galaxy formation and evolution can be considered through follow-up studies of DLA properties. Their metal abundances, for example, provide insight into the chemical evolution of the neutral gas over cosmic timescales. Follow-up studies at $z > 1.65$ generally rely on blind spectroscopic surveys for $\text{Ly}\alpha$, for which the $\text{Ly}\alpha$ line is shifted to optical wavelengths accessible from the ground (e.g. Prochaska et al. 2005 and references therein). However, these high-redshift DLAs only provide insight into the cosmic chemical evolution of neutral gas during the first third of the age of the universe (e.g. Pettini et al. 2002; Prochaska et al. 2003, 2007, and references therein).

At redshifts $z < 1.65$, Hubble Space Telescope (*HST*)-targeted searches for DLAs in strong MgII systems, like those found in SDSS spectra by Nestor et al. (2005), have resulted in significant numbers of lower-redshift DLAs being identified (e.g. RTN2006 and references therein). This has led to a growing sample of DLAs that have been used to determine cosmic neutral gas-phase metallicities at lower redshifts (e.g. Rao et al. 2005; Nestor et al. 2008, and references therein). However, the failure of the Space Telescope Imaging Spectrograph (STIS) onboard *HST* in 2004 has curtailed further lower-redshift DLA surveys. Moreover, lacking *HST* UV spectroscopy, follow-up metallicity studies of the lowest redshift population of DLAs have become impossible, given that the weak unsaturated metal lines that must be observed (Cr II, Fe II, Mn II, Si II, Zn II) lie in the UV when the redshifts are $z < 0.6$. Therefore, until the Cosmic Origins Spectrograph (COS) becomes available onboard *HST*, the best opportunities for measuring individual DLA metallicities at $z < 1.65$ lie at redshifts $z > 0.6$, for which the Zn II $\lambda\lambda 2026, 2062$ lines are shifted into the optical regime. In total there are currently only about 30 DLA systems with $0.6 < z < 1.65$ that can be used for individual metallicity studies.

Alternatively, an additional possibility is that DLA systems in the redshift interval $0.6 < z < 1.65$ might be identified by studying optical spectra and selecting systems which exhibit unusually strong metal-line absorption due to, e.g., Zn II. Such systems are representative of the highest metal-line column densities in the universe, and are likely to have H I column densities in the DLA

regime.

In this contribution, we successfully employ this second approach. After identifying a strong metal-line system at $z_{abs} \approx 1$ in the spectrum of SDSS QSO J0203–0910, we obtained follow-up NUV grism spectroscopy from the NASA Galaxy Evolution Explorer (*GALEX*) satellite to confirm our hypothesis that it is a DLA system. In particular, the damping wings on the Voigt profile of the observed Ly α line are strong and broad enough that N_{HI} is measurable even in the low-resolution *GALEX* NUV grism spectrum. This represents the first discovery of a DLA system by *GALEX*. Moreover, given that the metal lines of the absorption system are visible and measurable in the SDSS spectrum, our results also lead to a metallicity determination. This adds to the growing number of DLA metallicity measurements at $z < 1.65$.

The paper is laid out as follows. In §2, we present the *GALEX* data and our measurement of N_{HI} ; we also present the SDSS spectrum of QSO J0203–0910. We describe our measurements of the metal-line equivalent widths in §3. In §4 we derive and present the metal abundances of this system. We summarize our results in §5 and compare them to previous studies.

2. Observations

The SDSS QSO J0203–0910 was discovered in SDSS DR1 (Schneider et al. 2003; Richards et al. 2004). The QSO has SDSS u, g, r, i, and z magnitudes of 18.6, 18.3, 18.2, 18.0, and 18.0, respectively. This $z_{em} = 1.58$ QSO has a strong Mg II system along the sightline at $z_{abs} = 1.028$, with a rest equivalent width of $W_0^{\lambda 2796} = 2.66 \pm 0.06 \text{ \AA}$.¹ Since this line is saturated, the equivalent width is in fact an indication of the absorber’s velocity spread, or $\Delta v \approx 285 \text{ km s}^{-1}$.

We selected this system as a candidate DLA based on the relatively strong Zn II, Cr II, Mn II, and (some) Fe II absorption lines present in the SDSS spectrum (§2.2). It was approved for 31,500 sec of observation during Cycle 3 of *GALEX* (Program ID 0104).

2.1. *GALEX* Data

The *GALEX* grism spectra of SDSS QSO J0203–0910 (*GALEX* NUV mag = 19.8) were obtained in November 2007. The total exposure time of 30,720 sec was split between 16 visits. These data were processed, combined, and extracted in the standard pipeline procedure described by Morrissey et al. (2007). The resulting combined FUV-NUV spectrum is shown in Figure 1. The

¹Prochter et al. (2006) report $z_{abs} = 1.027$ and $W_0^{\lambda 2796} = 2.36 \text{ \AA}$.

spectrum has a signal-to-noise ratio of $S/N \approx 6$ per pixel in the region of the DLA at $\approx 2465 \text{ \AA}$, where the resolution of the spectrum is $R \approx 117$ with 6 pixels per resolution element.

In Figure 2 we show the normalized *GALEX* spectrum in the region of the $z_{abs} = 1.028$ Ly α absorption line. We fitted a local continuum to the spectral region using standard IRAF² routines. Since the absorption line lies in the Ly α forest, using a least-squares minimization to fit the line with a Voigt profile is not the best way to proceed. Instead, the line was fitted by eye with a Voigt profile convolved to the instrumental resolution following the procedure described in Rao & Turnshek (2000) and RTN2006. The placement of the continuum in the region of the absorption line is the primary source of N_{HI} uncertainty. To estimate the errors associated with the N_{HI} measurement, we shifted our estimate of the best-fit continuum level upward and downward by the 1σ error array and refit the DLA, as described in Rao & Turnshek (2000). The resulting column density determination is $N_{HI} = 1.5^{+0.4}_{-0.5} \times 10^{21}$ atoms cm^{-2} , which we report as $1.5 \pm 0.45 \times 10^{21}$ atoms cm^{-2} .

2.2. The SDSS QSO J0203–0910 Spectrum

The SDSS spectrum of QSO J0203–0910 was fitted using a cubic spline for the continuum and Gaussians for the broad emission features, as described in Nestor et al. (2005). For presentation, portions of the spectrum revealing the relevant metal lines are shifted into the rest frame of the absorber and normalized by the continuum fit; they are shown in the five panels of Figure 3. The figure caption notes which metal-line regions are covered.

3. Metal Absorption-Line Measurements

The rest equivalent width measurements of various unsaturated metal absorption lines (e.g. Zn II, Cr II, Mn II, and Fe II) in the $z_{abs} = 1.028$ system are presented in Table 1 (column 3). For completeness, Table 1 also includes measurements of saturated lines due to Mg II and Fe II. Note that the Fe II λ 2600 rest equivalent width, in combination with the Mg II λ 2796 rest equivalent width, makes the absorber a DLA candidate system according to the criterion of RTN2006. Details of measuring lines due to Zn II, Cr II, Mn II, and Fe II are discussed below since the results are used to determine metal abundances in §4.

²*IRAF* is distributed by the National Optical Astronomy Observatory, which is operated by the Association of Universities for Research in Astronomy (AURA) under cooperative agreement with the National Science Foundation.

3.1. Zn II and Cr II

We measured the equivalent widths of the metal lines in the normalized SDSS spectrum by fitting Gaussians to the absorption features using the ratios of relevant transition oscillator strengths, as presented by Nestor et al. (2003) (see their Table 2). The blends of Zn II and Mg I at 2026 \AA^3 and Cr II and Zn II at 2062 \AA are unresolved and were fitted by single Gaussians. The rest equivalent width of Zn II $\lambda 2026$ was found by subtracting the contribution due to Mg I $\lambda 2026$, as inferred from the measurement of the stronger Mg I $\lambda 2852$ line. The rest equivalent width of Cr II $\lambda 2062$ was inferred from the fit to Cr II $\lambda 2056$; it was subtracted from the measurement of the Cr II and Zn II 2062 \AA blend, resulting in the reported Zn II $\lambda 2062$ measurement. We note that the relatively large measured rest equivalent width of Cr II $\lambda 2066$ (oscillator strength $f = 0.0515$) seems anomalous given that it should be weaker than Cr II $\lambda 2056$ and Cr II $\lambda 2062$. Therefore, we have not used the Cr II $\lambda 2066$ measurement for the Cr^+ column density and abundance determinations reported in §4.

3.2. Mn II and Fe II

Measurements of some of the Mn II absorption lines at $z = 1.028$ are slightly complicated by Fe II absorption lines in a weaker Mg II system ($W_0^{\lambda 2796} = 0.442 \pm 0.057 \text{ \AA}$) at $z_{\text{abs}} = 1.217$. The Mn II $\lambda 2576$ line ($z = 1.028$) is unaffected, however Mn II $\lambda 2594$ ($z = 1.028$) is blended with Fe II $\lambda 2374$ ($z = 1.217$) and Mn II $\lambda 2606$ ($z = 1.028$) falls near Fe II $\lambda 2382$ ($z = 1.217$).

After measuring the absorption feature at the position of the Mn II $\lambda 2594$ ($z = 1.028$) and Fe II $\lambda 2374$ ($z = 1.217$) blend, we evaluated the contribution from Fe II as follows. We first measured the Fe II $\lambda 2344$ and Fe II $\lambda 2600$ lines in the $z = 1.217$ system, and used the relevant oscillator strengths to infer the Fe II $\lambda 2374$ ($z = 1.217$) rest equivalent width; its contribution is estimated to be $50 \pm 15 \text{ m\AA}$. We then subtracted this value from the total measured rest equivalent width of the Mn II and Fe II blend to obtain $W_0^{\lambda 2594} = 335 \pm 58 \text{ m\AA}$ ($z = 1.028$).

The Mn II $\lambda 2606$ line has the lowest oscillator strength of the three Mn II lines, $f = 0.1927$. Our measured value of this line, $W_0^{\lambda 2606} = 175 \pm 44 \text{ m\AA}$ ($z = 1.028$), is in agreement with the value predicted from the isolated Mn II $\lambda 2576$ line, $W_0^{\lambda 2606} = 185 \text{ m\AA}$. Also, the Fe II $\lambda 2382$ line ($z = 1.217$) and the Mn II $\lambda 2606$ line ($z = 1.028$) should be approximately resolved, given their $\approx 4 \text{ \AA}$ separation in the observed frame. We conclude, therefore, that the contribution of Fe II $\lambda 2382$ to the Mn II $\lambda 2606$ measurement is negligible.

There are five Fe II lines that can be measured in the SDSS spectrum, although only two of

³A Cr II line is also part of this blend, but its oscillator strength is so small that it was ignored (Nestor et al. 2003).

them, Fe II λ 2249 and Fe II λ 2260, appear to have equivalent widths placing them on the linear part of the curve of growth. Thus, these are the two most useful Fe II lines for column density determinations. It should be noted that the $z = 1.217$ Cr II lines at 2056 Å and 2066 Å are potential contaminants of the $z = 1.028$ Fe II lines at 2249 Å and 2260 Å, respectively. However, inspection of the SDSS spectrum indicates no evidence for Zn II λ 2026 absorption or a Zn II λ 2062 and Cr II λ 2062 absorption blend at $z = 1.217$. Given this, we conclude that any Zn II or Cr II features at $z = 1.217$ are too weak to produce a significant detection in the SDSS spectrum; they would certainly lie well within the reported measurement errors for the Fe II λ 2249 and Fe II λ 2260 lines at $z = 1.028$.

4. Column Densities and Element Abundance Determinations

With the exception of the Cr II λ 2066 measurement described above, but which we ignore, the other rest equivalent width measurements appear to be in reasonable agreement. The rest equivalent widths of the weak lines due to Zn II, Cr II, Mn II, and two of the Fe II lines can be converted directly into column densities since they are unsaturated and lie on the linear part of the curve of growth.

Column density results for these ions are presented in Table 1 (column 4) next to the first transition of each ion; the results are weighted averages derived from all of the relevant rest equivalent widths in column 3, unless otherwise noted. Table 1 also lists the N_{HI} value determined from the *GALEX* spectrum. The various column densities are used to derive the element abundance results discussed below. When we quote abundances relative to solar values, we use the solar values of Grevesse & Sauval (1998) as compiled in Table 2 of Rao et al. (2005).

It is generally agreed that most of the Zn and Cr is singly ionized in the neutral DLA regions (Howk & Sembach 1999); this should hold for singly ionized Fe and Mn as well. Under this assumption, we have converted the Zn⁺, Cr⁺, Mn⁺, and Fe⁺ column densities into the neutral gas-phase abundances. We find that [Zn/H] = -0.69 ± 0.22 , or $\approx 20\%$ solar; [Cr/H] = -1.07 ± 0.18 and [Fe/H] = -1.03 ± 0.16 , both $\approx 9\%$ solar; and [Mn/H] = -1.48 ± 0.17 , or $\approx 3\%$ solar. These results are given in Table 1 (column 5).

Also in Table 1 (column 6), we give the elemental abundances of Zn, Cr, and Mn relative to Fe, expressed as [X/Fe]. We find [Zn/Fe] = 0.34 ± 0.15 and [Cr/Fe] = -0.04 ± 0.07 . The value [Cr/Zn] = -0.38 ± 0.17 is typically taken as an indication of the presence of dust, given that Cr is expected to be readily depleted onto grains, whereas Zn is not (Pettini, Boksenberg, & Hunstead 1990). The same holds for the inferred value of [Fe/Zn]. Thus, from the measurements we can infer that $\approx 60\%$ of the Cr (and Fe) is depleted onto grains. This value is comparable to [Cr/Zn] ≈ -0.5 found for the

Milky Way halo (Savage & Sembach 1996). Nestor et al. (2003) found $[\text{Cr}/\text{Zn}] = -0.64 \pm 0.13$ in a composite SDSS spectrum for a sample of Mg II absorbers with $W_0^{2796} \geq 1.3 \text{ \AA}$ and $0.9 \leq z \leq 1.3$. With regard to Mn, we also find that $[\text{Mn}/\text{Fe}] = -0.45 \pm 0.16$. This result is similar to that found in previous DLA metallicity studies (e.g., Pettini et al. 2000; Ledoux, Bergeron, & Petitjean 2002; Rao et al. 2005); it has been suggested to be due to metallicity-dependent production of Mn (see §5).

5. Summary & Discussion

Based on the presence of unusually strong metal lines (Zn II, Cr II, Mn II, and two low-oscillator-strength Fe II lines) at $z_{\text{abs}} = 1.028$ in the SDSS spectrum of QSO J0203–0910, we selected the system as a DLA absorber candidate. We obtained a *GALEX* NUV grism spectrum to confirm the presence of the DLA, and found $N_{\text{HI}} = 1.5_{-0.5}^{+0.4} \times 10^{21} \text{ atoms cm}^{-2}$. This marks the first discovery of a DLA system by *GALEX*. Using the existing SDSS spectrum, we determined the system’s metal-line column densities from measurements of the unsaturated metal lines.

As discussed further below, the Zn^+ column density in this system is among the highest known. Therefore, prior to our *GALEX* observation, we also thought that this system might be a good candidate for a solar or super-solar metallicity DLA system. However, we found $[\text{Zn}/\text{H}] = -0.69 \pm 0.22$, or $\approx 20\%$ solar, which is within the normal range for DLA systems at this redshift.

Measurements of absorption lines due to Cr II and Fe II in this system indicate that the gas-phase abundance of Cr and Fe is lower than Zn, with $\approx 60\%$ of the Cr and Fe depleted onto grains. In addition, measurements of the Mn II lines indicate that, relative to solar, the gas-phase abundance of Mn is even less than that of Cr and Fe. This may be due to a combination of depletion and an early stage of chemical evolution for the absorbing gas. In particular, it is agreed that $[\text{Mn}/\text{Fe}]$ is clearly underabundant (e.g. $[\text{Mn}/\text{Fe}] < -0.2$) in low-metallicity stars (e.g. $[\text{Fe}/\text{H}] < -1$), but then $[\text{Mn}/\text{Fe}]$ starts to increase with increasing $[\text{Fe}/\text{H}]$ (McWilliam, Rich, & Smecker-Hane 2003, and references therein). However, the details of the origin of Mn production, and the roles of SNeIa and SNeII enrichment, are still debated (e.g. Feltzing, Fohlman, & Bensby 2007; Bergemann & Gehren 2008, and references therein).

Our value for the Zn^+ column density, $\log N_{\text{Zn}^+} \approx 13.16 \pm 0.15$, places it right at the empirical threshold of $\log N_{\text{Zn}^+} < 13.15$ on a plot of $[\text{Zn}/\text{H}]$ vs. $\log N_{\text{HI}}$, above which DLAs have generally not been found (Boissé et al. 1998; Meiring et al. 2006). Herbert-Fort et al. (2006) have classified DLAs above this threshold, i.e., with $\log N_{\text{Zn}^+} \geq 13.15$, as “metal-strong.” This soft limit has been suggested as being due to obscuration by dust (e.g. Boissé et al. 1998), however more recent results suggest that the lack of systems above this limit is due more to their inherent rarity

(Herbert-Fort et al. 2006, and references therein).

The strong metal lines in this system, nevertheless, are not indicative of an unusually large metallicity compared to other DLAs at $z \approx 1$. For example, Kulkarni et al. (2007) found $\langle [\text{Zn}/\text{H}] \rangle = -0.82 \pm 0.15$ for 20 DLAs with $0.1 < z < 1.2$, which is consistent with our result. Rather, the strong metal lines in this system can be attributed to its large H I column density. As noted above, this DLA does have a relatively high metallicity in comparison to systems with similar N_{HI} .

Our metallicity results may also be compared to those determined at $z > 0.6$ from SDSS composite spectra. For example, in an analysis of one composite created from 90 Mg II absorbers with $W_0^{\lambda 2796} > 1.3 \text{ \AA}$ and $0.9 < z < 1.35$, many of which should be DLAs (Rao & Turnshek 2000; RTN2006), Nestor et al. (2003) estimated a metallicity of $[\text{Zn}/\text{H}] = -0.56 \pm 0.19$. Turnshek et al. (2005) reported an extension of this analysis using a much large sample of strong Mg II absorbers with $1 \lesssim z \lesssim 2$, and parameterized $[\text{Zn}/\text{H}] = -0.4 - 0.0043 e^{[(6 - W_0^{\lambda 2796})/0.88]}$ for $0.6 \text{ \AA} \leq W_0^{\lambda 2796} \leq 6.0 \text{ \AA}$. Using our measured value of $W_0^{\lambda 2796} = 2.66 \text{ \AA}$ for the Mg II absorber corresponding to the DLA in SDSS QSO J0203–0910, this parameterization would predict $[\text{Zn}/\text{H}] = -0.59$, in agreement with our measured value of $[\text{Zn}/\text{H}] = -0.69 \pm 0.22$.

Candidate DLA selection based on strong lines of Zn II remains the best chance for finding solar or super-solar metallicity DLAs at $z \approx 1$. We suspect that such a system might exhibit a Zn^+ column density similar to the $z_{\text{abs}} = 1.028$ system, but have $N_{\text{HI}} \approx 2 \times 10^{20} \text{ atoms cm}^{-2}$, i.e., right at the DLA N_{HI} lower threshold. The presence of other normally weak lines may also provide a clue, but many of the other elements are subject to depletion. Larger surveys using *HST* COS will permit an evaluation of the success of this technique at $0.6 \leq z \leq 1.65$.

We thank Daniel Nestor and Anna Quider for their contributions which helped produce the Pittsburgh SDSS Mg II QSO absorption-line catalog. E.M.M gratefully acknowledges support from NASA/GALEX Guest Investigator grant NNX 08AJ87G. D.A.T and S.M.M. acknowledge support from NASA/GALEX Guest Investigator grant NNX 08AE20G.

Funding for the SDSS and SDSS-II has been provided by the Alfred P. Sloan Foundation, the Participating Institutions, the National Science Foundation, the U.S. Department of Energy, the National Aeronautics and Space Administration, the Japanese Monbukagakusho, the Max Planck Society, and the Higher Education Funding Council for England. The SDSS Web Site is <http://www.sdss.org/>.

The SDSS is managed by the Astrophysical Research Consortium for the Participating Institutions. The Participating Institutions are the American Museum of Natural History, Astrophysical Institute Potsdam, University of Basel, University of Cambridge, Case Western Reserve University, University of Chicago, Drexel University, Fermilab, the Institute for Advanced Study, the Japan

Participation Group, Johns Hopkins University, the Joint Institute for Nuclear Astrophysics, the Kavli Institute for Particle Astrophysics and Cosmology, the Korean Scientist Group, the Chinese Academy of Sciences (LAMOST), Los Alamos National Laboratory, the Max-Planck-Institute for Astronomy (MPIA), the Max-Planck-Institute for Astrophysics (MPA), New Mexico State University, Ohio State University, University of Pittsburgh, University of Portsmouth, Princeton University, the United States Naval Observatory, and the University of Washington.

REFERENCES

- Bergemann, M., & Gehren, T. 2008, *A&A*, 492, 823
- Boissé, P., Le Brun, V., Bergeron, J., & Deharveng, J.-M. 1998, *A&A*, 333, 841
- Feltzing, S., Fohlman, M., & Bensby, T. 2007, *A&A*, 467, 665
- Grevesse, N., & Sauval, A. 1998, *Space Sci. Rev.*, 85, 161
- Herbert-Fort, S., Prochaska, J.X., Dessauges-Zavadsky, M., Ellison, S.L., Howk, J.C., Wolfe, A.M., & Prochter, G.E. 2006, *PASP*, 118, 1077
- Howk, J.C., & Sembach, K.R. 1999, *ApJ*, 523, L141
- Kulkarni, V.P., Khare, P., Péroux, C., York D.G., Lauroesch, J.T., & Meiring, J.D. 2007, *ApJ*, 661, 88
- Ledoux, C., Bergeron, J., & Petitjean, P. 2002, *A&A*, 385, 802
- McWilliam, A., Rich, R.M., & Smecker-Hane, T.A. 2003, *ApJ*, 592, L21
- McWilliam, A., Rich, R.M., & Smecker-Hane, T.A. 2003, *ApJ*, 593, L145 (erratum)
- Meiring, J.D., Kulkarni, V.P., Khare, P., Bechtold, J., York, D.G., Cui, J., Lauroesch, J.T., Crotts, A.P.S., & Nakamura, O. 2006, *MNRAS*, 370, 43
- Morrissey et al. 2007, *ApJS*, 173, 682
- Nestor, D.B., Rao, S.M., Turnshek, D.A., & Vanden Berk, D. 2003, *ApJ*, 595, L5
- Nestor, D.B., Turnshek, D.A., & Rao, S.M. 2005, *ApJ*, 628, 637
- Nestor, D.B., Pettini, M., Hewett, P.C., Rao, S., & Wild, V. 2008, *MNRAS*, 390, 1670
- Pettini, M., Boksenberg, A., & Hunstead, R.W. 1990, *ApJ*, 348, 48

- Pettini, M., Ellison, S.L., Steidel, C.C., & Shapley, A.E. 2000, ApJ, 532, 65
- Pettini, M., Ellison, S.L., Bergeron, J., & Petitjean, P. 2002, A&A, 391, 21
- Prochaska, J.X., Gawiser, E., Wolfe, A.M., Cooke, J., & Gelino, D. 2003, ApJS, 147, 227
- Prochaska, J.X., & Herbert-Fort, S. 2004, ApJ, 116, 622
- Prochaska, J.X., Herbert-Fort, S., & Wolfe, A.M. 2005, ApJ, 635, 123
- Prochaska, J.X., Wolfe, A.M., Howk, J.C., Gawiser, E., Burles, S.M., & Cooke, J. 2007, ApJS, 171, 29
- Prochter, G.E., Prochaska, J.X., & Burles, S.M. 2006, ApJ, 639, 766
- Rao, S., & Turnshek, D. 2000, ApJS, 130, 1
- Rao, S.M., Prochaska, J.X., Howk, J.C., & Wolfe, A.M. 2005, AJ, 129, 9
- Rao, S.M., Turnshek, D.A., & Nestor, D.B. 2006, ApJ, 643, 75 (RTN2006)
- Richards, G.T., et al. 2004 ApJS, 155, 257
- Savage, B.D., & Sembach, K.R. 1996, ARA&A, 34, 279
- Schneider, D.P., et al. 2003, AJ, 126, 2579
- Turnshek, D.A., Rao, S.M., Nestor, D.B., Belfort-Mihalyi, M., & Quider, A.M. 2005, in IAU Colloq. 199, *Probing Galaxies through Quasar Absorption Lines*, ed. P. Williams, C. Shu, & B. Ménard (Cambridge: Cambridge Univ. Press), 104
- Wolfe, A.M., Turnshek, D.A., Smith, H.E., & Cohen, R.D. 1986, ApJS, 61, 249
- Woosley, S.E., & Weaver, T.A. 1995, ApJS, 101, 181

Table 1. Absorption Line Measurements: SDSS QSO J0203–0910, $z = 1.028$

Ion	λ_{rest} (Å)	W_0 (mÅ)	$\log N$ (cm^{-2})	[X/H]	[X/Fe]
H I	1215.67	...	$21.18^{+0.11}_{-0.16}$
Zn II	2026.14	306 ± 91	13.16 ± 0.15	-0.69 ± 0.22	0.34 ± 0.15
	2062.66	92 ± 65			
Cr II	2056.25	235 ± 50	13.78 ± 0.07^a	-1.07 ± 0.18	-0.04 ± 0.07
	2062.23	175 ± 37			
	2066.16	381 ± 63			
Fe II	2249.88	371 ± 53	15.65 ± 0.03^b	-1.03 ± 0.16	...
	2260.78	396 ± 44			
	2344.21	1287 ± 35			
	2374.46	1108 ± 34			
	2382.77	1791 ± 33			
	2586.65	1430 ± 46			
	2600.17	1780 ± 45			
Mn II	2576.88	337 ± 44	13.23 ± 0.05	-1.48 ± 0.17	-0.45 ± 0.16
	2594.50	335 ± 58^c			
	2606.46	176 ± 45			
Mg I	2026.48	27 ± 2			
	2852.96	890 ± 56			
Mg II	2796.35	2265 ± 56			
	2803.53	2450 ± 62			

^aCalculated from Cr II $\lambda 2056$, $\lambda 2062$

^bCalculated from Fe II $\lambda 2249$, $\lambda 2260$

^cBlend with weak Fe II $\lambda 2374$ line at $z_{abs} = 1.217$

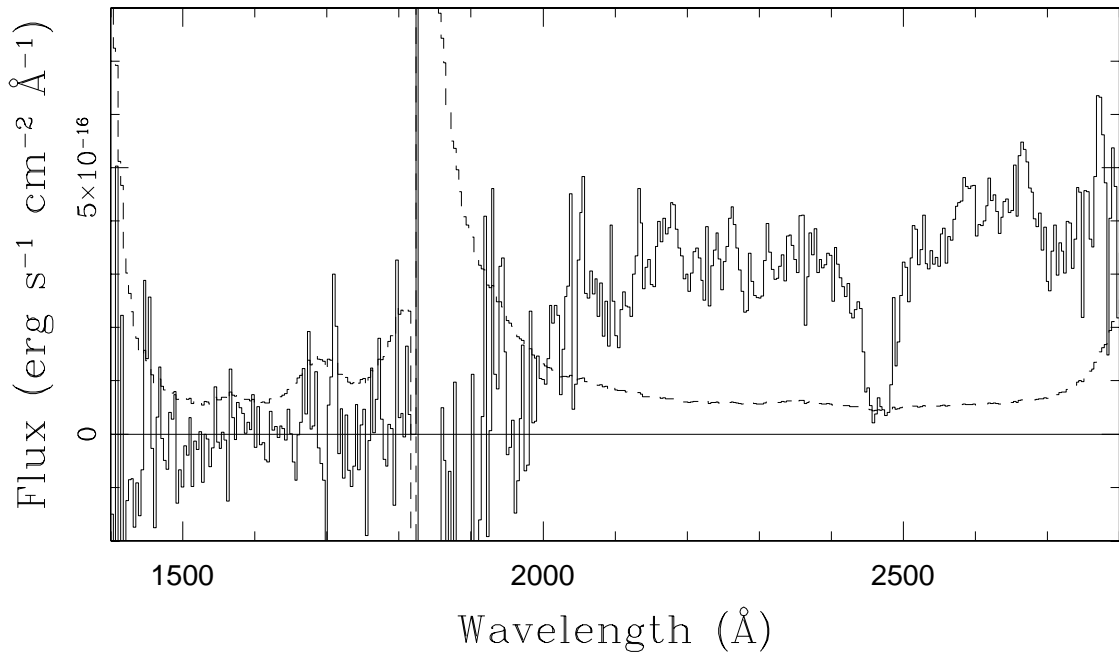


Fig. 1.— The complete *GALEX* FUV-NUV grism spectrum of SDSS QSO J0203–0910. The $z_{abs} = 1.028$ Ly α absorption line is clearly visible near 2465 Å. The dashed line is the 1- σ error array. The FUV and NUV spectra meet at 1750 Å, where the detectors have minimal sensitivities. The drop in sensitivity of the detectors and the Lyman limit of this absorber (at ≈ 1850 Å) are responsible for the spike in the error array and the absence of flux in the FUV channel.

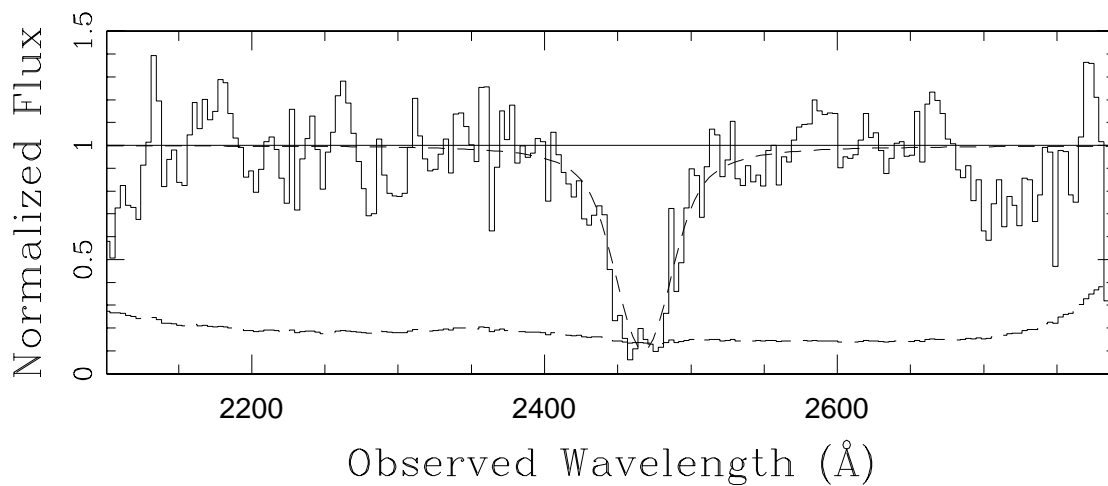


Fig. 2.— The normalized observed-frame *GALEX* NUV grism spectrum of SDSS QSO J0203–0910 and the Ly α absorption line at $z_{abs} = 1.028$. The line has been fitted with a Voigt profile having column density $N_{HI} = 1.5 \times 10^{21}$ atoms cm^{-2} and convolved with the *GALEX* NUV grism resolution. The horizontal dashed curve is the 1σ error array.

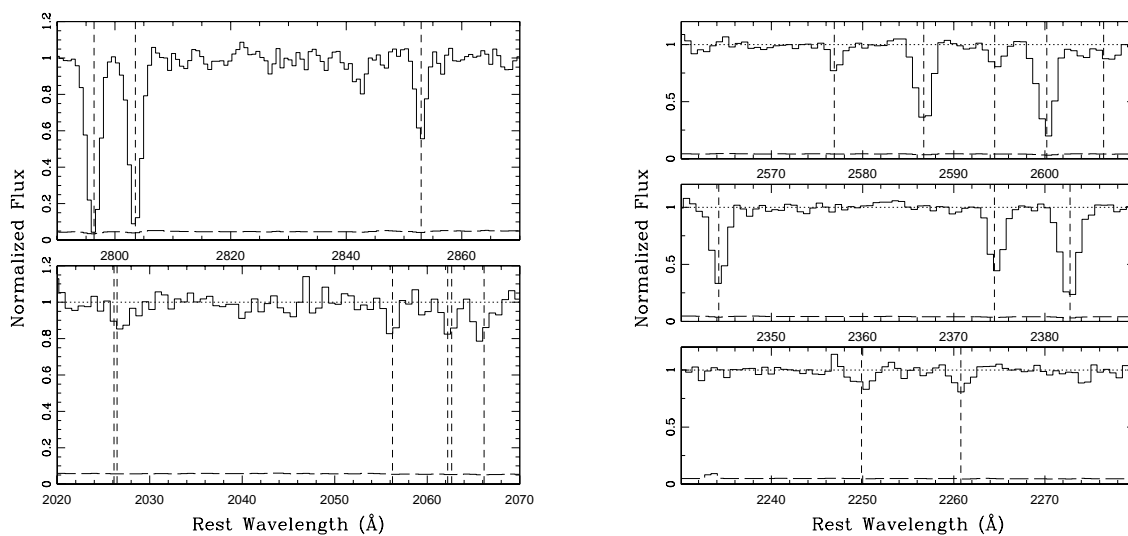


Fig. 3.— These portions of the normalized spectrum of SDSS QSO J0203–0910 show selected absorption lines due to metals in the rest frame of the $z = 1.028$ absorber. See Table 1 for the rest wavelengths of the various absorption lines marked by vertical dashed lines. The spectra are unsmoothed, and the horizontal dashed curves show the 1σ error array. The two panels on the left side show the regions containing the strong Mg II doublet and the Mg I line (top panel) and the Zn II, Mg I, and Cr II lines (bottom panel). The three panels on the right side show the regions containing Mn II and strong Fe II lines (top panel), other strong Fe II lines (middle panel), and weak Fe II lines (bottom panel).